Title	Chaotic motion of microplugs under high-frequency thermocapillary actuation
Author(s)	Jiao, Zhenjun; Nguyen, Nam-Trung; Huang, Xiaoyang
Citation	Jiao, Z. J, Nguyen, N. T., & Huang, X. Y. (2007). Chaotic motion of microplugs under high-frequency thermocapillary actuation. Journal of Micromechanics and Microengineering, 17(1), 180-185.
Date	2007
URL	http://hdl.handle.net/10220/7849
Rights	© 2007 IOP Publishing Ltd. This is the author created version of a work that has been peer reviewed and accepted for publication by Journal of Micromechanics and Microengineering, IOP Publishing Ltd. It incorporates referee's comments but changes resulting from the publishing process, such as copyediting, structural formatting, may not be reflected in this document. The published version is available at: [http://dx.doi.org.ezlibproxy1.ntu.edu.sg/10.1088/0960-1317/17/1/023].

Chaotic motion of micro plugs under high-frequency thermocapillary actuation

Zhenjun Jiao,Nam-Trung Nguyen§,Xiaoyang Huang

† School of Mechanical and Aerospace Engineering, Nanyang Technological University, 50 Nanyang Avenue, Singapore 639798

Abstract. This paper reports experimental results on chaotic motion of liquid plugs under high-frequency thermocapillary actuation. In the experiments, two heaters were alternately activated. The liquid plug was positioned in a glass capillary between these two heaters. The periodic temperature gradients generated by the two heaters made the liquid plug to move back and fort. The images of the plug were captured by a camera. Plug position a customized image processing programme. The results were recorded as time series for further analysis. The nonlinear motion of the liquid plug in a glass capillary was systematically investigated with tools coming from chaotic dynamics. Phase-space portraits are reconstructed from time series of the plug position obtained in the experiments. The results show that the limit sets formed by the phase space trajectories are attractors. The largest Lyapunov exponent and correlation dimension of these attractors are calculated and indicate that these attractors are chaotic. A chaotic plug motion has potential applications in fluid mixing inside liquid plugs of capillary-based microfluidics. External chaotic motion could improve mixing in liquid plugs of capillary-based lab-on-a-chip platforms.

§ To whom correspondence should be addressed (mntnguyen@ntu.edu.sg)

1. Introduction

Recent development trend shows that droplet-based or digital microfluidics is a promising alternative for traditional continuous-flow microfluidics. Microplugs and microdroplets formed in channels can be used as transport vessels and a reaction platforms for lab-on-a-chip applications. Active manipulation of microdroplets or microplugs is an important task for these new reaction platforms. Active manipulation of droplets can be achieved by modulation of surface stresses [1, 2]. For instance, active transport of microdroplets was achieved by electrowetting [3, 4]. Furthermore, the thermocapillary effect is another method for modulation of surface stresses. Brozoska et al. [5], Darhuber et al. [6] and Tseng et al. [7] studied the motion of a droplet on a flat surface under the influence of a temperature field. Recently, we reported an one-dimensional (1-D) analytical model for the transient behavior of a liquid droplet in a capillary which is heated at one end [8] and at two ends [9].

Deoxyribonucleic acid (DNA) processing systems based on liquid plugs in glass capillary was previously reported by Friedman and Meldrum [10]. In this capillary-based platform, mixing inside a liquid plug is an important task. Evensen et al. used pneumatic force induced by an external piezoelectric actuator [11]. They pointed out that mixing relies much on the deposition and collection of the liquid film on the capillary wall as the liquid plug is driven back and fort. Thus, the plug motion is important for mixing in liquid plugs of capillary-based platforms. Recently, Chen et al. keep chemicals and reaction products as liquid plugs in a glass capillary for storage and postprocessing [12]. We previously have demonstrated both theoretically and experimentally that these liquid plugs stored inside a glass capillary can be manipulated using external heaters [9]. This method is based on thermocapillary effect with two alternately activated heaters. This method has a potential in manipulating not only the plug motion but also the flow field inside the plug. In the previous work, periodic motions induced by relatively slow switching frequencies were investigated. In this paper, we demonstrate that chaotic motion of the plug can be achieved with a higher switching frequency. The chaotic plug motion would have a big impact on the mixing process in side the plug.

Since early 1980s, research on nonlinear dynamics of physical systems has been matured [13, 14]. A number of techniques and methods for detecting chaotic dynamic behaviors have been developed. The physical system of our previous experiment [9] was described by two coupled differential equations, one for the spreading of temperature in the capillary wall and another one for the plug motion. This coupled partial differential equation system indicates the possibility of a chaotic system. In fact, we have observed previously that the motion of the plug becomes irregular when the switching frequency was relatively high. At lower frequencies ($f < 0.1$ Hz), the plug follows the change of temperature and the plug motion is periodic. In the current study, the position and the velocity of the plug was automatically captured and converted into a time series using a customized image-processing programme. The times series of the position can be analysed to prove the chaotic characteristics of the plug motion. In the current

study, we first performed experiments to investigate the nonlinear behavior of plug movement under high switching frequency ($0.1 \leq f \leq 1$). After getting the time series of the plug position, nonlinear dynamical analysis methods such as phase portraits, Lyapunov exponents, and fractal dimensions were applied to the measured time series. The analysis results prove the chaotic characteristics of the plug motion under this actuation condition.

2. Chaotic motion based on thermocapillary actuation

Figure 1 illustrates schematically the actuation concept and the corresponding experimental setup. The thermocapillary actuation concept was described previously by a coupled model [9]. Two heaters created a periodic temperature gradient in a glass capillary. The liquid plug is placed between the two heaters. The temperature gradient across the liquid plug drives it back and fort, following the periodic change of the temperature field. Increasing the switching frequency ($f \geq 0.1$ Hz) leads to an irregular plug motion, Figure 2. Our previous has shown that measured results agree well with analytical results for low switching frequencies $f < 0.1$ Hz. The plug behavior depends on coupling of two first-order dynamic systems: the thermal system of the glass capillary and the mass-damping system of the liquid plug itself. At high switching frequencies, the coupling of these two dynamic systems become unstable leading to possible chaos. Based on experimental data, we will prove that the motion of the liquid plug at high switching frequencies is indeed chaotic.

One of the important features of chaos is the sensitive dependence on initial conditions (SDIC). Small changes in the initial state of a system can grow at an exponential rate and then dominates the behavior of the system. SDIC can be quantified with Lyapunov exponents, which are the longtime average exponential rates of divergence of nearby states. If a system has at least one positive Lyapunov exponent, the system is chaotic. The larger the positive exponent, the more chaotic the system will be. In a system there might be any number of Lyapunov exponents, however, we only need to find out that the largest one is positive to confirm chaos. Hence, estimation of the dominant exponent is especially important. Recently many experiments in different fields have demonstrated that chaos is common in non-equilibrium systems. In these experiments the systems have totally different physical mechanisms and levels of complexity but the chaotic behaviors mathematically are often similar [13, 14]. Therefore we can use the same technique for different types of experiments with the results which is experimentally measured time series. In order to identify chaotic motions from experimentally measured time series, the most often used methods are are phase portraits, Lyapunov exponents, and fractal dimensions. Following, all these three methods are applied to our experimental results.

3. Materials and methods

Details on the experimental setup were described previously [9], Fig. 1. The experiments were carried out with a glass capillary, which has an outer diameter of $D_o = 1.39$ mm, an inner diameter of $D_{in} = 0.95$ mm and a length of $L_c = 150$ mm. The density. the conductivity and the specific heat of glass are assumed to be $\rho = 2500$ kg/m^3, $\kappa = 1.4$ W/mK and $c = 750$ J/m^3, respectively. The working liquid is silicone oil with a dynamic viscosity of $\nu = 10Cst$, a surface tension of $\sigma = 20.1$ mN/m, a density of $\rho = 930$ kg/m^3. The distance between the two heaters was about $L_c = 8$ mm. In all experiments, the heating power of both heaters were kept at about 2 W by monitoring and adjusting the applied voltage and current. The current was switched between the two heaters by the circuit shown in Fig. 1. Position measurement started only when the whole system is thermally in a quasi-steady-state condition. The image frames were captured long after the whole system is switched on. The frame rate of the charge coupled device (CCD) camera was kept at 10 frames per switching period throughout all experiments. The inserts in Fig. 1 show the typical images of the moving plug. The recorded images were subsequently processed by a customized software written in Matlab to extract the time function of the plug position.

Figure 2 shows the time function of the position of a 1-mm long plug at a switching frequencies of 0.1 Hz, 0.4 Hz, 0.8 Hz and 1 Hz. The results show that the position obviously has an irregular behavior. The plug does not follow the switching frequency of the temperature field. At high frequencies, unstable behavior is dominant due to the small movement magnitude, the relatively small driving force and the short switching period. Uncertainties in forces such as the damping viscous force become dominant at high-frequency, low-magnitude actuation. Autocorrelation functions of the time series depicted in Fig. 2 are calculated according to:

$$A(\tau) = \frac{\sum_{i=1}^{N}(x_{i+\tau} - \bar{x})(x_i - \bar{x})}{\sum_{i=1}^{N}(x_i - \bar{x})^2} \tag{1}$$

Figure 3 shows the corresponding autocorrelation functions of the time series depicted in Fig. 2. Autocorrelation function (ACF) is a basic technique used in analyzing of time series. ACF helps to determine how quickly signals or processes change with respect to the time and whether a process has a periodic component. The autocorrelation function will have its largest value $A = 1$ at $\tau = 0$. This peak can appear again,it the time series is periodic. The signal in Fig. 3(a) is obviously periodic. ACF is used later for determining the time delay for constructing the phase portrait and determining the Lyapunov exponent as well as the fractal dimension.

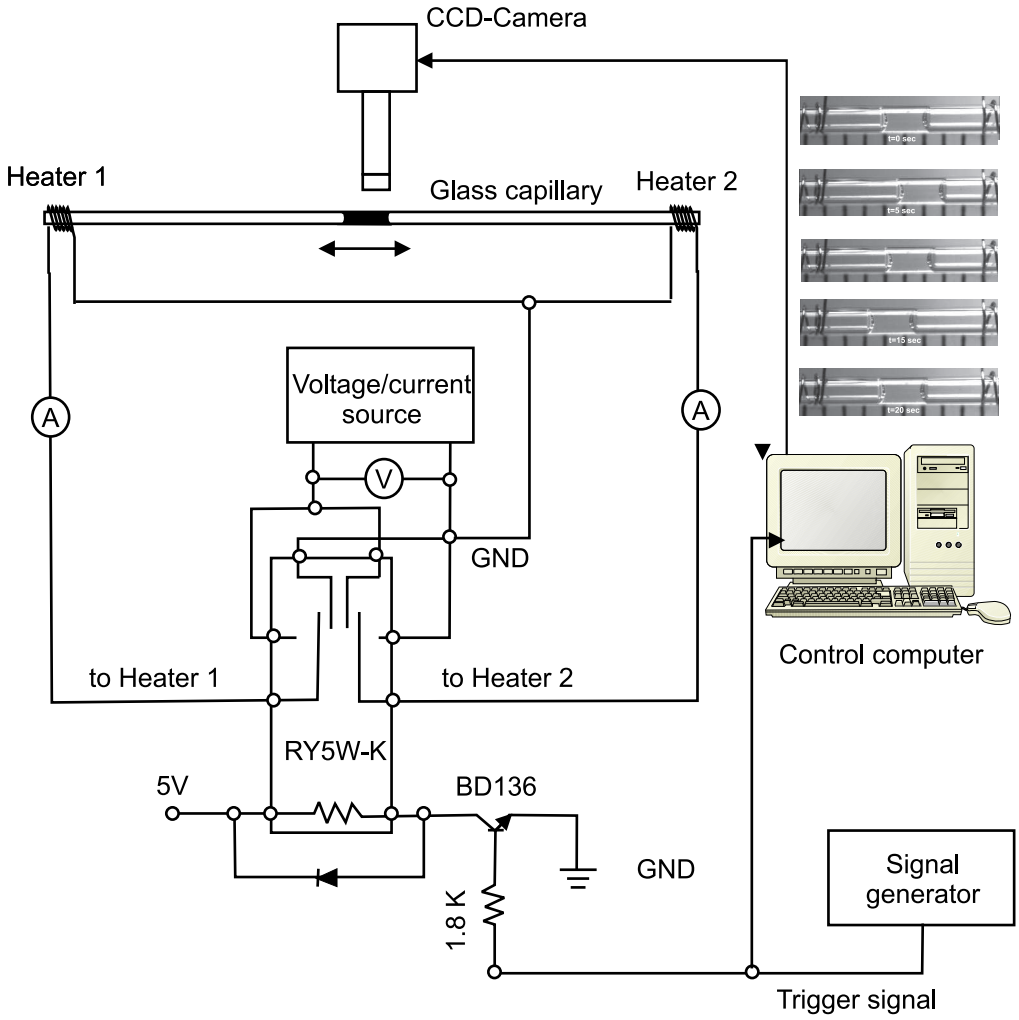

Figure 1. Experimental setup for characterization of the plug movement

4. Phase portrait from time series

The dynamical equations of a physical system can often be written in the following form:

$$\frac{\mathrm{d}X(i)}{\mathrm{d}t} = G\left[X(i)\right] \tag{2}$$

where $X(i)$ is an n-component vector in the phase space of the system, and G stands for n nonlinear functions of these components. It is well-known that much could be learned about dynamical behavior of a system from analysing the trajectories in the phase space. For a practical physical system, the phase space often has a large number of components, i.e., the dimension of the phase space is very large. However, most dynamical systems involve only a small number of important degrees of freedom. In practice, the study can often be restricted to a low-dimensional phase space which only includes these important degrees of freedom. Such a phase space is usually called embedded phase space. In most experimental investigations, only time series of a single variable of the system can be measured. The time-delay technique is used to reconstruct

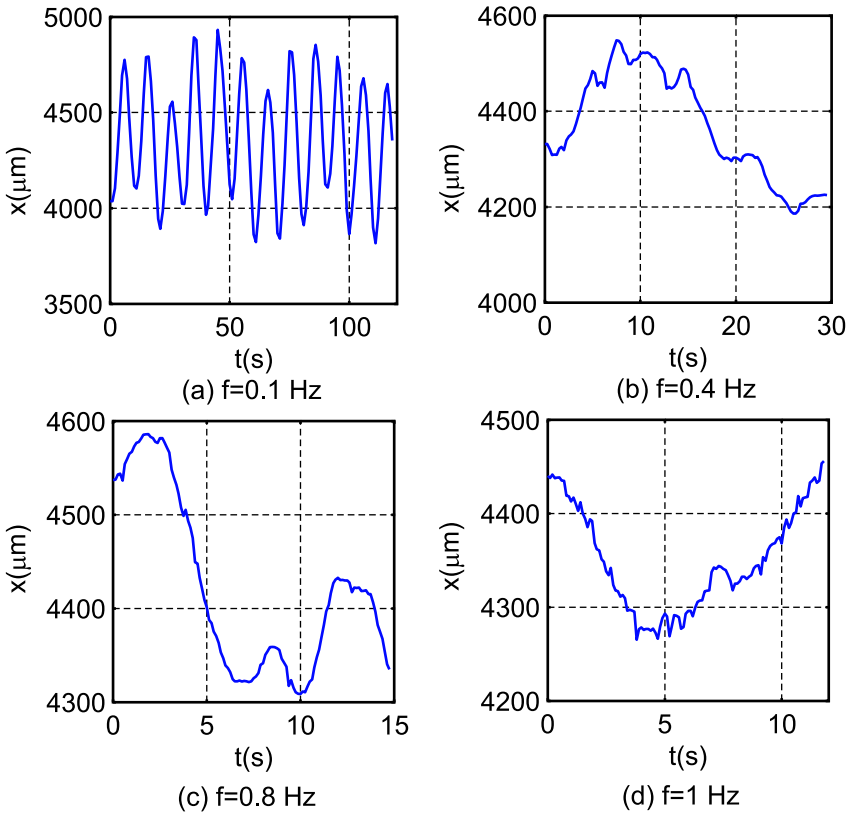

Figure 2. Time signal of plug position at (a) $f = 0.1$ Hz, (b) $f = 0.4$ Hz, (c) $f = 0.8$ Hz and (d) $f = 1$ Hz

multidimensional phase portraits from this time series, in order to examine the dynamic properties of the whole system. Take a N-point position time series $x(i)$ as the example; the reconstructed trajectory, X, can be expressed as a matrix:

$$X = (X_1,\ X_2,\ X_3, \ldots X_M)^T \tag{3}$$

where where $X_k,\ k = 1, 2, ..., M,$ is the state of the system at discrete time k, and is given by

$$X_k = (X_k,\ X_{k+J},\ \ldots X_{k+(m-1)J}), k = 1, 2, ..., M \tag{4}$$

where J is the time delay on reconstruction delay, and m is the embedding dimension. The integers M, N, m, and J satisfy the following equation:

$$M = N - (m - 1)J \tag{5}$$

Thus, an m-dimension phase portrait can be reconstructed from the time series of position $x(i)$. The embedding dimension m is usually estimated in accordance with Taken's theorem, i.e., $m > 2n$, where n is the dimension of the attractor [15–21]. It has been shown that if the embedding dimension m is sufficiently large, the pseudo-phase portrait constructed by the method of time delays will in principle have the same properties as a phase portrait constructed from the independent variables [15–21]. For visualization of

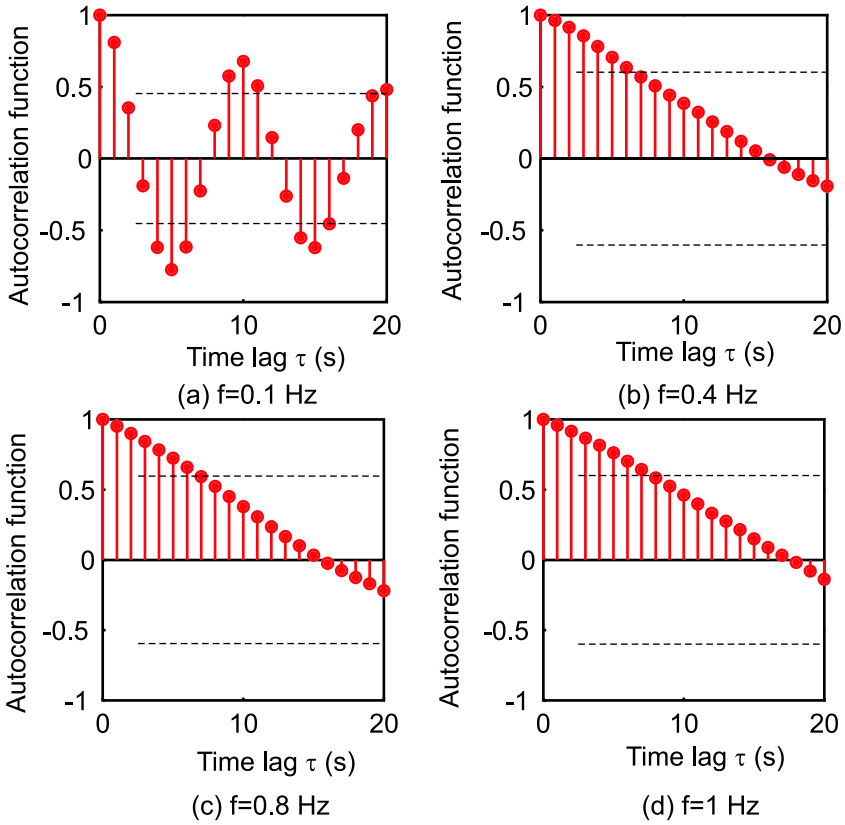

Figure 3. Autocorrelation function of the time series depicted in Fig. 2 (the two dashed lines in each diagram indicate the approximate upper and lower confidence bounds): (a) $f = 0.1$ Hz, (b) $f = 0.4$ Hz, (c) $f = 0.8$ Hz and (d) $f = 1$ Hz

the reconstructed phase portrait, $m = 2$ or $m = 3$ is often used, while higher m is used for the further study to determine the largest Lyapunov exponent and fractal dimension of the attractor. The choice of the time delay J is almost but not completely arbitrary. A good approximation of J is equal to the discrete time lag where the autocorrelation function of the time series drops to $(1 - 1/e)$ of its initial value.

In the present study, the embedding dimension $m = 2$ and the time delays $J = 4$ are used to obtain the phase portraits. According to the ACF shown in Fig. 3, the value of J is equal to the discrete time lag τ where the autocorrelation function drops to $1 - 1/e$ [15] of its initial value. Due to the small number of data points in our experiment, the value for the time delay is chosen as $J = 4$. In our customized Matlab programme, the positive integer of discrete values, beyond which the theoretical ACF is effectively 0, was chosen to be 40. The two dashed lines in each diagram of Fig. 3 indicate the approximate upper and lower confidence bounds. As the time series has 120 data points, the other 80 ACF values confidently lie between these two dashed lines.

Two-dimensional vectors $X_k = (x_k, x_{k+J})$, $k = 1, 2, ..., M$, are constructed from the time series data $x(i)$. Figure 4 shows the two-dimensional phase portraits obtained by plotting $x(i+J)$ versus $x(i)$ for $J = 4$. The time series data were measured at $f = 0.1$ Hz,

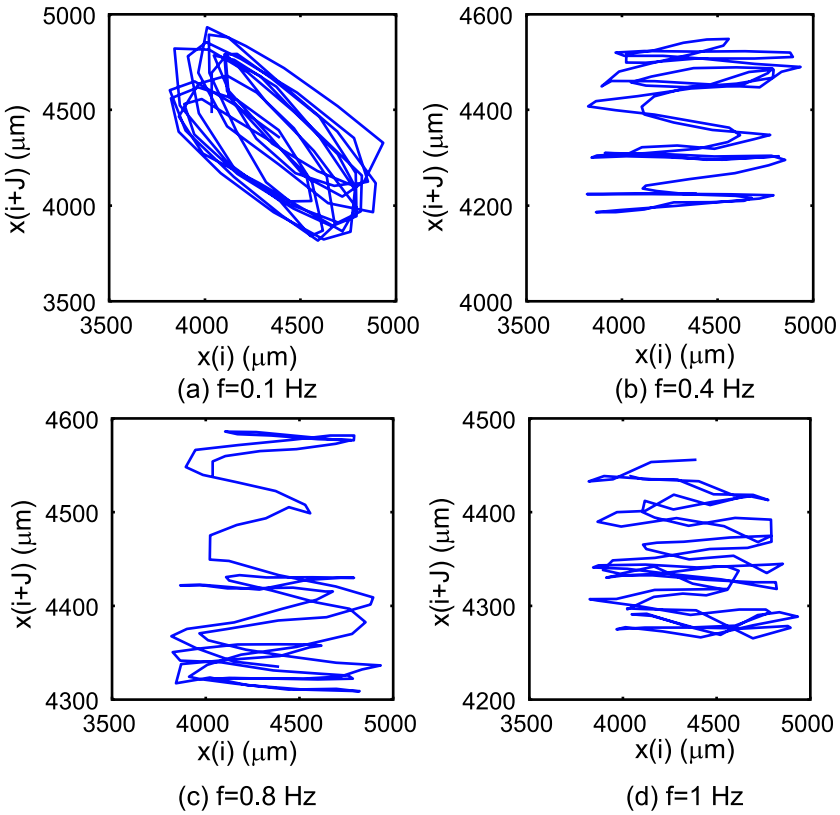

Figure 4. Phase portrait constructed from the position measured at a time lag of $J = 4$: (a) $f = 0.1$ Hz, (b) $f = 0.4$ Hz, (c) $f = 0.8$ Hz and (d) $f = 1$ Hz.

$f = 0.4$ Hz, $f = 0.8$ Hz and $f = 1$ Hz. In these phase portraits, it can be seen that the trajectories lie on a limit set in the embedded phase space for each time delay, which demonstrates that these phase portraits are attractors. Following, Lyapunov exponents and fractal dimensions are determined to prove that these attractors are strange or chaotic.

5. Lyapunov exponents and fractal dimensions

The most widely used criteria to quantify chaos in a system are the Lyapunov exponents and the fractal dimensions. Positive Lyapunov exponents indicate the sensitive dependence on initial conditions. If a system has at least one positive Lyapunov exponent, the system is chaotic. A system may possess many Lyapunov exponents, but only the largest Lyapunov exponent needs to be checked in order to confirm chaos.

The fractal dimension is a non-integer dimension which is a hallmark of a chaotic attractor. There are many types of definitions and measures of fractal dimensions, of which the correlation dimension is the commonly used one. There are many algorithms that are applicable to estimate the largest Lyapunov exponent from time series [15, 17]. The method used in the present paper was developed by Rosenstein et al. [15]. This method is fast, easy to implement, and robust to changes in parameters such as the

embedding dimension, the size of data set, the reconstruction delay, and the noise level. Furthermore, the correlation dimension can also be calculated simultaneously.

The largest Lyapunov exponent of a chaotic attractor is defined in the following equation:

$$d(t) = Ce^{\lambda_1 t} \tag{6}$$

where $d(t)$ is the average divergence of trajectories with nearby initial conditions on the attractor at time t, C is a constant that normalizes the initial separation, and λ_1 is the largest Lyapunov exponent.

The first step of Rosenstein's algorithm involves reconstructing the attractor dynamics from a single time series by using the method described above. The algorithm then locates the nearest neighbor of each point on the trajectories. The nearest neighbor, U_j is found by searching for the point that minimizes the distance to the particular reference point $\hat{j}$. This can be expressed as

$$d_j(0) = \min \|X_j - X_{\hat{j}}\|, j = 1, 2, 3...M \tag{7}$$

where $dj(0)$ is the initial distance from the j-th point to its nearest neighbor, $\|..\|$ denotes the Euclidean norm, and M is the number of reconstructed vectors in the phase space. The largest Lyapunov exponent is then estimated as the mean rate of separation of the nearest neighbors [20, 21].

Let the nearest neighbors evolute with time along the trajectories and assume that the j-th pair of nearest neighbors diverges approximately at a rate given by the largest Lyapunov exponent:

$$d_j(t) = C_j e^{\lambda_1 (i\Delta t)}, j = 1, 2, 3...M \tag{8}$$

where C_j is the initial separation, i is the discrete time with which the nearest neighbors evolute, and Δt is the time interval between samples. Taking the logarithm of both sides of (8) yields:

$$\ln d_j(i) = \ln C_j + \lambda_1 (i\Delta t), j = 1, 2, 3...M \tag{9}$$

Equation (9) represents a set of approximately parallel lines for $j = 1, 2, ..., M$, with a slope proportional to λ_1 . Taking the average of $\ln d_j(i)$ over all values of j, the largest Lyapunov exponent λ_1 then equals to the slope of a line defined by:

$$\langle \ln d_j(i) \rangle = \lambda_1 (i\Delta t), j = 1, 2, 3...M \tag{10}$$

where $\langle\rangle$ denotes the average over all values of j.

Figure 5 shows the plots of $\langle \ln dj(i) \rangle$ versus the time $t = (i\Delta t)$. The solid lines are the calculated results, and the dashed lines are the fitting functions based on the least-square method. The largest Lyapunov exponent λ_1 is equal to the slope of the dashed lines. The analyzed time series $x(i)$ is the same as presented in the previous

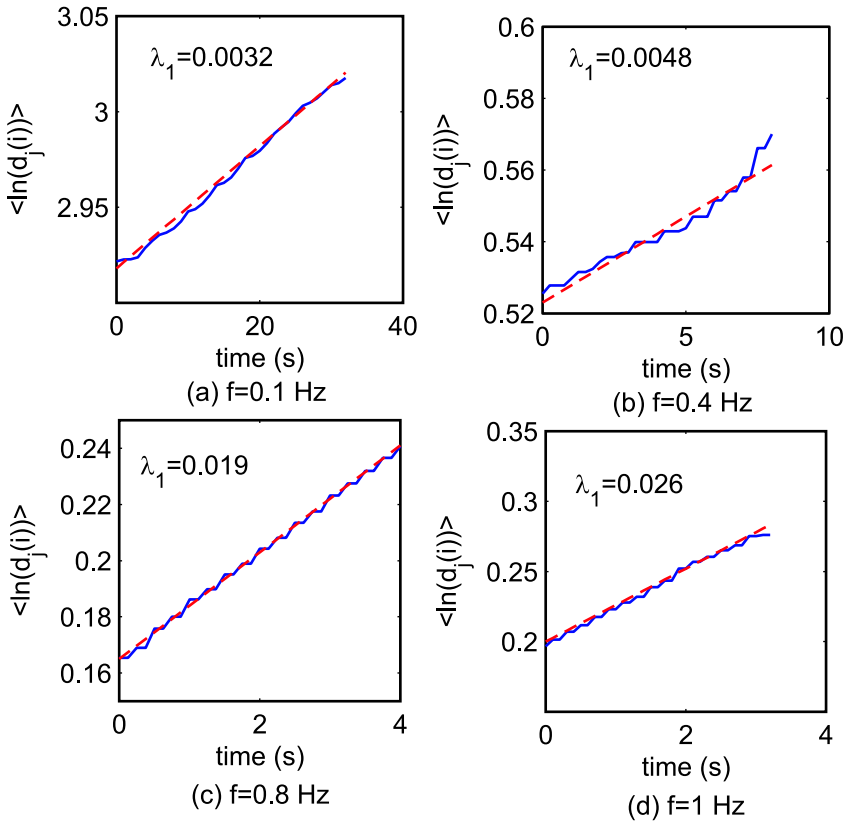

Figure 5. $\ln d_j(i)$ versus time ($m = 10$, $J = 4$, the dashed lines are the fitting functions) for (a) $f = 0.1$ Hz; (b) $f = 0.4$ Hz; (c) $f = 0.8$ Hz; (d) $f = 1$ Hz.

sections. The embedding dimension remains constant at $m = 10$. The calculated largest Lyapunov exponents is $\lambda_1 = 0.01$ when the switching frequency is $f = 1$ Hz. The positive largest Lyapunov exponents indicate that the attractors are chaotic. With increasing positive Lyaunove exponents from 0.0032 at 0.1 Hz to 0.026 at 1Hz, the results prove the existence of chaos in the plug motion at high switching frequencies.

The next important quantitative measure of an attractor is the correlation dimension. The correlation dimension estimates the complexity of a system, which can be determined from the correlation function $C(R)$. Let R denote a small positive value; for a reconstructed attractor X, the two-point correlation function is defined as [24]:

$$C(R) = \frac{1}{M(M-1)} \sum_{i=1}^{M} \sum_{j \neq 1}^{M} \theta[R - d(X_i - X_j)] \tag{11}$$

where M is the number of the reconstructed vectors, θ is the Heaviside function, and $d(X_i - X_j)$ represents the distance between two m-dimensional vectors. The Euclidean norm can be used to measure the distance between two vectors. $C(R)$ is interpreted as the fraction of pairs of points that is separated by a distance less than or equal to R. The correlation dimension of an attractor is defined in the following equation:

$$C(R) = \lim_{R \to 0} a R^{D_c} \tag{12}$$

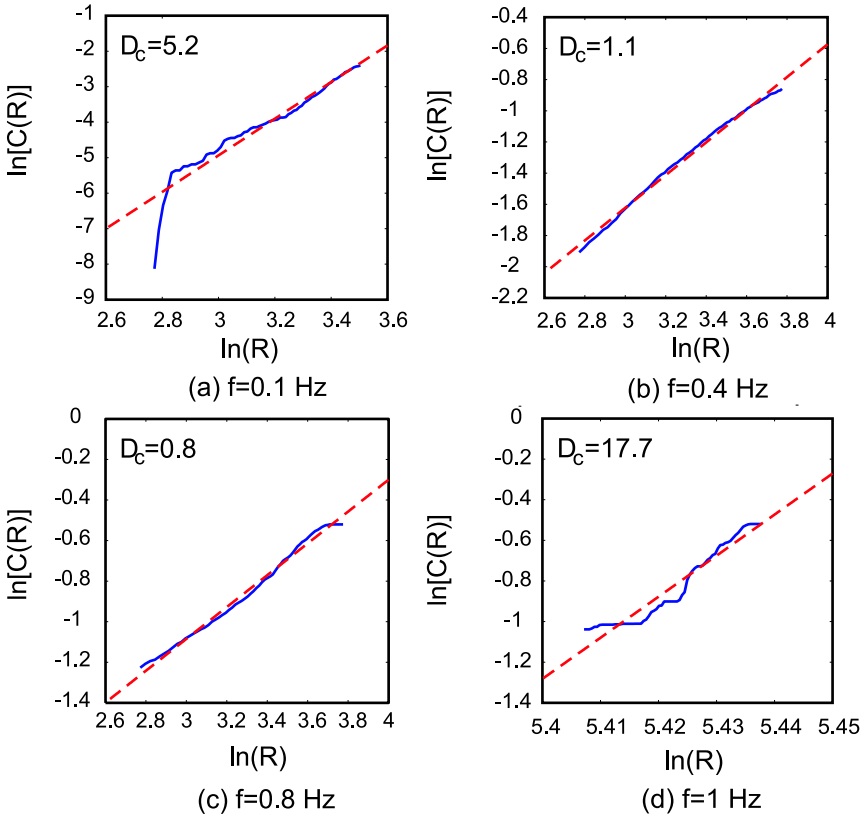

Figure 6. $\log C(R)$ versus $\log R$ ($m = 10$, $J = 4$, the dashed lines are the fitting functions) for: (a)$f = 0.1$ Hz, (b) $f = 0.4$ Hz, (c) $f = 0.8$ Hz, and (d) $f = 1$ Hz.

where a is a constant value, D_c is the correlation dimension, and J is the time delay. The correlation dimension can now be estimated from the slope of the linear part of the $\log C(R)$ versus $\log(R)$ curve according to

$$D_c = \frac{\mathrm{d}\log[C(R)]}{\mathrm{d}\log(R)} \tag{13}$$

Figure 6 shows the curves of $\log[C(R)]$ versus $\log(R)$ for the different switching frequencies. The solid lines are the calculated results. The dashed lines are the fitting functions. The correlation dimension is determined by the slope of the dashed line. Embedding dimension m is taken equal to 10. The results show that the system has non-integer dimensions, which means that the attractors depicted in Fig. 4 are chaotic.

6. Conclusion

The chaotic motion of a liquid plug under high-frequency thermocapillary actuation was investigated. The measured time series data of the position were analysed by constructing the phase-space portraits, evaluating the largest Lyapunov exponent and calculating the fractal dimension. The results show that the phase-space trajectories define a limit set in the phase space that is an attractor. This attracting set is chaotic, because nearby trajectories separate exponentially. Moreover, the fractal dimension of

the attractor has also been calculated, which gives the degree of the system complexity. The results indicate the potential use of chaotic plug motion to improve mixing in capillary-based microfluidics. The The same heating concept can be used for realizing polymerase chain reaction (PCR) of DNA as reported before by Friedman and Meldrum [10]. Thus a complete DNA processing system using glass capillaries can potentially designed and entirely based on thermal actuation and control. Our future work will focus on the flow and mixing pattern inside the liquid plug.

Acknowledgment

N. T. Nguyen would like to thank the Agency of Science, Technology and Research, Singapore (A*Star, SERC grant No. 0521010108 'Droplet-based micro/nanofluidics') for its financial support. Z. Jiao thanks the Nanyang Technological University for a research scholarship.

References

[1] Darhuber A A and Troian S M 2005, Principles of microfluidic actuation by modulation of surface stresses *Ann. Rev. Fluid Mech.* **37**, 425–455
[2] Atencia G and Beebe D J 2005, Controlled microfluidic interfaces *Nature* **437**, 648–655
[3] Pollack M G, Fair R B and Shenderov A D 2000, Electrowetting-based actuation of liquid droplets for microfluidic applications *Applied Physics Letter* **77**, 1725–1727
[4] Ren H R, Fair B and Pollack M G 2004, Automated on-chip droplet dispensing with volume control by electro-wetting actuation and capacitance metering *Sensors Actuators B* **98**, 319–327
[5] Brozoska J B, Brochard-Wyart F and Rondelez F 1993, Motions of droplets on hydrophobic model surfaces induced by thermal gradients *Langmuir* **9**, 2220–2224
[6] Darhuber AA, Davis JM and Troian SM 2003, Thermocapillary actuation of liquid flow on chemically patterned surfaces *Physics of Fluidcs*, **15**, 1295–1304
[7] Tseng YT, Tseng FG, Cheng YF and Chieng CC 2004, Fundamental studies on micro-droplet movement by Marangoni and capillary effects *Sensors and Actuators A* **114**, 292–301
[8] Nguyen NT and Huang X 2005, Thermocapillary effect of a liquid plug in transient temperature field *Japanese Journal of Applied Physics* **94**, 1139–1142
[9] Jiao Z, Nguyen N T, Huang X Y and Ang Y Z 2006, Reciprocating thermocapillary plug motion in an externally heated capillary *Microfluidics and Nanofluidics*, in print
[10] Fiedman N A and Meldrum D R 1998, Capillary tube resistive thermal cycling *Analytical Chemistry*, **70**, 2997–3002
[11] Evensen H T, Meldrum D R and Cunningham D L 1998, Automated fluid mixing in glass capillaries *Review of Scientific Instruments*, **69**, 519–526
[12] Chen D L , Gerdts C J and Ismagilov R F 2005, Using microfluidics to observe the effect of mixing on nucleation of protein crystals *Journal of American Chemical Society* **127**, 9672–9673
[13] Strogatz S H and Addison-Wesley 1996, Nonlinear Dynamics and Chaos, Singapore.
[14] Moon F C and Wiley 1992, Chaotic and Fractal Dynamics, New York.
[15] Rosenstein M T, Collins J J, and Luca C J D 1993, A practical method for calculating largest Lyapunov exponents from small data sets *Physica D* **65**, 117–134
[16] Takens F 1981, Lecture Notes in Mathematics *Springer*, Berlin, 366–381
[17] Wales D J 1991, Calculating the rate of loss information from chaotic time series by forecasting *Nature* London **350**, 485–488

[18] Lauterborn W and Cramer E 1981, Subharmonic route to chaos observed in acoustics *Phys. Rev. Lett* **47**, 1445–1447

[19] Cabeza C, Sicardi-Schifino A C, Negreira C, and Montaldo G 1998, Experimental detection of a subharmonic route to chaos in acoustic cavitation through the tuning of a piezoelectric cavity *J. Acoust. Soc. Am.* **103**, 3227–3229

[20] Nayfeh A H and Tsai M S 1974, Nonlinear wave propagation in acoustically lind ducts *J. Sound Vib.* **35**, 77–89

[21] Packard N H, Crutchfield J P, Farmer J D, and Shaw R S 1980, Geometry from time series *Phys. Rev. Lett.* **45**, 712–716

[22] Wolf A, Swift J B, Swinney H L, and Vastano J A 1985 , Determining Lyapunov exponents from a time series *Physica D* **16**, 285–317

[23] Sato S, Sano M, and SawadaY 1987, Practical methods of measuring the generalized dimension and the largest Lyapunov exponent in high dimensional chaotic systems *Prog. Theor. Phys.* **77**, 1–5

[24] Abarbanel H D I, Brown R, and Kadtke J B, Prediction in chaotic nonlinear systems: Methods for time series with broadband Fourier spectral *Phys. Rev. A* **41**, 1782–1807